Gene Therapy (2014) **21**, 10–18
© 2014 Macmillan Publishers Limited All rights reserved 0969-7128/14
www.nature.com/gt

OPEN

ORIGINAL ARTICLE

Efficient siRNA transfection to the inner ear through the intact round window by a novel proteidic delivery technology in the chinchilla

W Qi[1], D Ding[2], H Zhu[3], D Lu[4], Y Wang[3], J Ding[3], W Yan[1], M Jia[1] and Y Guo[1]

The use of small-interfering RNA (siRNA) has great potential for the development of drugs designed to knock down the expression of damage- or disease-causing genes. However, because of the high molecular weight and negative charge of siRNA, it is restricted from crossing the blood–cochlear barrier, which limits the concentration and size of molecules that are able to gain access to cells of the inner ear. Intratympanic approaches, which deliver siRNA to the middle ear, rely on permeation through the round window for access to the structures of the inner ear. We developed an innovative siRNA delivery recombination protein, TAT double-stranded RNA-binding domains (TAT-DRBDs), which can transfect Cy3-labeled siRNA into cells of the inner ear, including the inner and outer hair cells, crista ampullaris, macula utriculi and macula sacculi, through intact round-window permeation in the chinchilla *in vivo*, and there were no apparent morphological damages for the time of observation. We also found that Cy3-labeled siRNA could directly enter spiral ganglion neurons and the epithelium of the stria vascularis independently; however, the mechanism is unknown. Therefore, as a non-viral vector, TAT-DRBD is a good candidate for the delivery of double-stranded siRNAs for treating various inner ear ailments and preservation of hearing function.

Gene Therapy (2014) **21,** 10–18; doi:10.1038/gt.2013.49; published online 10 October 2013

Keywords: TAT double-stranded RNA-binding domains; small-interfering RNA; transfection; inner ear; chinchilla

INTRODUCTION

RNA interference (RNAi) is a remarkable endogenous regulatory pathway that can lead to sequence-specific gene silencing and was discovered by Fire *et al.*[1] It is a natural ubiquitous cellular mechanism for small-RNA-guided post-transcriptional suppression of gene expression. RNAi can be activated exogenously by introducing synthetic double-stranded small-interfering RNAs (siRNAs) directly into the cytoplasm or by expression through viral vectors of short hairpin RNAs that are processed intracellularly into small RNAs that mimic the endogenous gene-silencing siRNAs.[2,3] The short double-stranded siRNAs integrate with RNA-induced silencing complex in the cytoplasm, where they are separated into single strands. One strand guides the cleavage of target mRNAs by Argonaute2 in a sequence-homology-dependent manner.[4] Dicer is a vital endonuclease that belongs to the RNase III family and can precisely cleave double-stranded RNA into 21- to 23-bp nucleotides with characteristic termini: the 3′-end carries a dinucleotide overhang, whereas the 5′-end terminates in a monophosphate group. The length and termini features of siRNA are important for efficient recognition by and combination with the RNA-induced silencing complex.[5–7] The RNA-induced silencing complex is triggered by the introduction of an active RNAi effector, and the delivery of such an effector to a cell brings about potent and specific knockdown of its target gene. Theoretically, siRNA can be designed for any gene of interest based on its mRNA sequence. Such unlimited potential has made RNAi a favorite gene knockdown strategy in mammalian cells.[8] As a result, there has been a significant surge of interest in the application of siRNA in functional genomics studies; furthermore, this approach has shown impressive therapeutic potential that is expected to be realized in the near future.

Otologic clinical and research practice requires the delivery of drugs, including siRNAs, into the inner ear. To be effective in the inner ear, siRNAs must reach their target cells that express the genes of interest. A potent gene-silencing agent has no utility if it cannot be delivered to its intended cell type, tissue or organ. Delivery of siRNAs *in vivo* is the biggest obstacle faced by RNAi application.[8,9] For the inner ear, although the presence of the blood–labyrinth barrier limits wanted or unwanted systemic diffusion of transfer agents, the cochlea is still considered to be a particularly attractive target organ for the study and potential application of gene therapy involving RNAi. The intratympanic approach, which delivers therapeutics to the middle ear by permeation through the round-window membrane (RWM) for access to the structures of the inner ear, has great potential in both research and clinically.[10–12] The cochlea is a very complicated, enclosed space, and its function is sensitive to small changes in fluid (endolymph and perilymph) volume. Therefore, in comparison with intracochlear methods, which allow for direct insertion of drugs into the inner ear, the latter undermines the integrity of the labyrinth and is thus associated with a risk of irreversible damage to the inner ear. It may not be suitable for clinical practice.

Liposomes and a few viral vectors can follow pathways for the diffusion of small molecules such as siRNA across the RWM.[10] To date, data regarding the cytotoxicity of liposomes are

[1]Department of Otolaryngology, Huashan Hospital Fudan University, Shanghai, China; [2]Center for Hearing and Deafness, State University of New York at Buffalo, Buffalo, NY, USA; [3]Novoprotein Scientific Inc, Shanghai, China and [4]State Key Laboratory of Genetic Engineering, School of Life Sciences, Fudan University, Shanghai, China. Correspondence: Dr W Qi, Department of Otolaryngology, Huashan Hospital Fudan University, 12 Urumqi road, Shanghai 200040, China.
E-mail: weidongqi@gmail.com
Received 17 March 2013; revised 21 July 2013; accepted 27 August 2013; published online 10 October 2013

a

MGRKKRRQRRRGHSGRKKRRQRRRGHIYPYDVPDYA
GDPGRKKRRQRRRGDPAGDLSAGFFMEELNTYRQKQ
GVVLKYQELPNSGPPHDRRFTFQVIIDGREFPEGEGRS
KKEAKNAAAKLAVEILNKELEHHHHHH

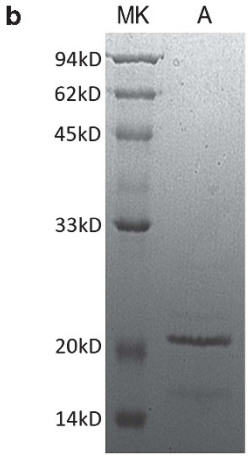

Figure 1. (**a**) TAT-DRBD characterization, single-letter amino acid sequence and domain demarcation of TAT-DRBD: TAT-TAT-HA-TAT-BRBD-6xHis. (**b**) SDS-polyacrylamide gel electrophoresis of TAT-DRBD protein (lane A, final product; MK, molecular weight standards).

inadequate, which limits their practical application.[13–15] Transduction efficiency with cationic liposomes through the RWM to the inner ear is low, and the effect is transient.[16] Most commercially available cationic liposome/lipid-based systems mediate significant non-specific downregulation of the total cellular protein content at optimal doses for specific gene silencing,[14] and almost all of the commercial cationic lipids and polymers induce some cytotoxicity.[17] In addition, recent work demonstrated that some cationic lipids can agonize Toll-like receptor 4 and induce interferons and proinflammatory cytokines.[18] Moreover, virus-based delivery systems such as lentivirus, adenovirus and adeno-associated virus, while efficient, may be fatally flawed due to safety concerns, because they induce mutations and trigger immunogenic and inflammatory responses.[19] As a result, extensive work has focused on the development of efficacious non-viral delivery systems, including direct chemical modification of siRNA, nanoparticles and so on. These novel strategies provide ways to safely overcome obstacles facing RNAi.

Dramatic developments in gene engineering have led to the design and generation of functional peptides and proteins for basic research and clinical uses. Peptide transduction domains, also called cell-penetrating peptides, have great potential for the rapid translocation of various molecular substances from small molecular compounds to nano-sized particles, large fragments of DNA into cells, and show enhanced cellular uptake *in vitro* and *in vivo* in a non-cytotoxic manner via macropinocytosis, a specialized type of fluid-phase endocytosis performed by all cells.[20–23] $TAT_{48–57}$(GRKKRRQRRR) is a type of peptide transduction

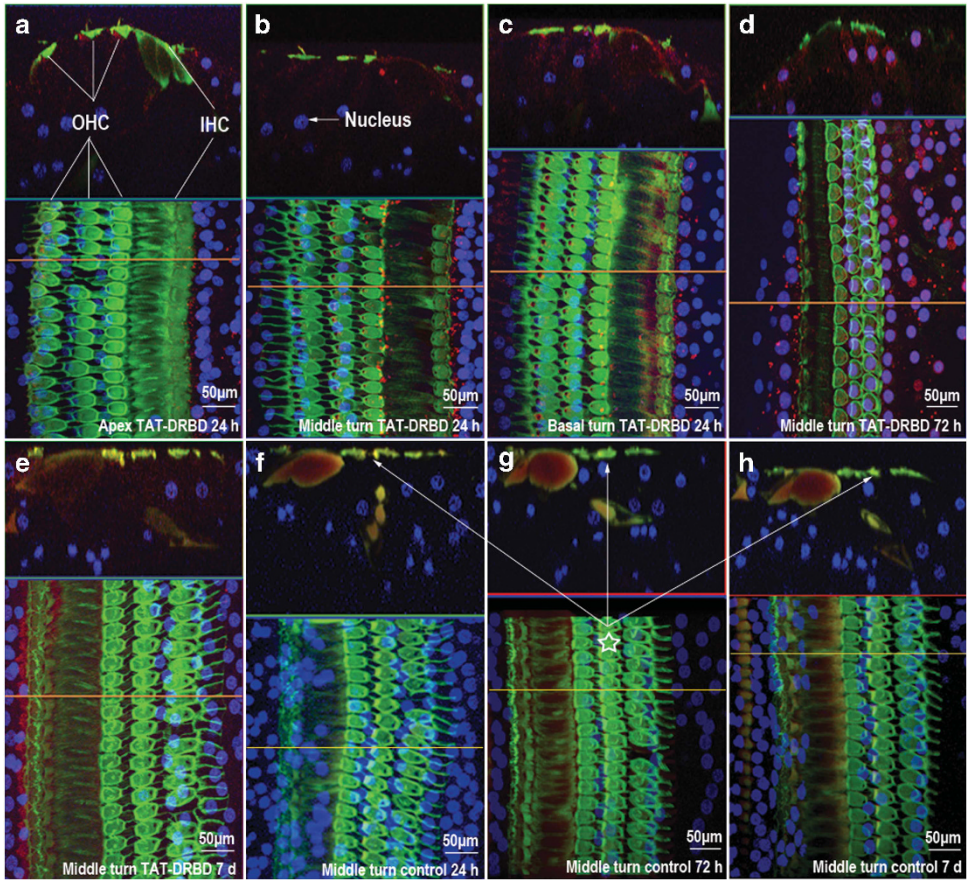

Figure 2. Photomicrographs of basilar membrane hair cells transfected with Cy3-labeled siRNA (red) and stained with Alexa Fluor 488 Phalloidin (green) and To-Pro-3 (blue). The red fluorescence of Cy3-labeled siRNAs was present in the cytoplasm of all cochlear inner hair cells and outer hair cells from the apex (**a**) to the middle turn (**b**) and basal turn (**c**) 24 h after transfection with TAT-DRBD. The signal was still present after 48 h (**d**) but was only slightly attenuated after 7 days (**e**). Cy3 fluorescence was not detected in control ears after 24 h (**f**), 72 h (**g**) and 7 days (**h**); the red fluorescence of Cy3 ('☆') was only found on the membrane of hair cells from longitudinal section photomicrographs but could not be found in the cytoplasm.

© 2014 Macmillan Publishers Limited

domain and TAT fusion protein that can conjugate with siRNAs and internalize siRNAs efficiently through macropinocytosis[24,25] or through direct penetration without endocytosis.[26,27] In some cases, however, the TAT–siRNA complex achieved neither efficient internalization nor effective silencing of protein expression.[20] In addition, few data showed that direct conjugation of a cationic TAT to an anionic siRNA results in neutralization and precipitation of the molecules with poor delivery and cytotoxicity.[23] Therefore, the key to successful use of peptide transduction domain delivery is masking the negative charge of siRNA. Double-stranded RNA-binding domains (DRBD) can bind to double-stranded RNAs with high avidity ($K_D \sim 10^{-9}$)[28] but not to single-stranded RNA, single-stranded DNA or double-stranded DNA, and regulate signaling events and gene expression in cells,[28,29] thereby masking their negative charge. Dowdy and colleagues[23,30] constructed a TAT protein fusion with a DRBD. The DRBD masked the negative charge of the siRNA, allowing the TAT to efficiently deliver siRNA into cells. They found that TAT-DRBD delivery of siRNAs induced rapid RNAi in a large percentage of various primary and transformed cells with no apparent cytotoxicity, minimal off-target transcriptional changes and no induction of innate immune responses.

One important consideration will be to determine a method that provides uniform distribution of transfer throughout the entire cochlea with minimal damage due to siRNA application in the inner ear. We created the TAT-DRBD fusion protein based on the amino acid sequence and domain demarcation of TAT-DRBD using a DNA recombination technique, and placed it onto the intact round window of a chinchilla *in vivo*. Therefore, the purpose of this study was to compare siRNA transfection efficiency at different time points in various target cells of the inner ear, including hair cells of the Organ of Corti, spiral ganglion, crista ampullaris, macula utriculi, macula sacculi and stria vascularis, and determine the kinetic profiles with or without TAT-DRBD.

RESULTS

TAT-DRBD protein generated using a DNA recombination technique

TAT-DRBD fusion protein was created using a DNA recombination technique. First, through chemosynthesis of the target double-stranded DNA fragment, a DNA sequence corresponding to the single-letter amino acid sequence and domain demarcation of TAT-DRBD along with the TAT-TAT-HA-TAT-DRBD-6xHis (TAT: TAT_{48-57}, DRBD: PKR_{9-78}; Figure 1a) arrangement was generated.[30] Next, enzyme cleavage, connection to PET30a vector and transformation into competent *Escherichia coli* DH5α cells were performed. After screening for positive clones and sequencing,

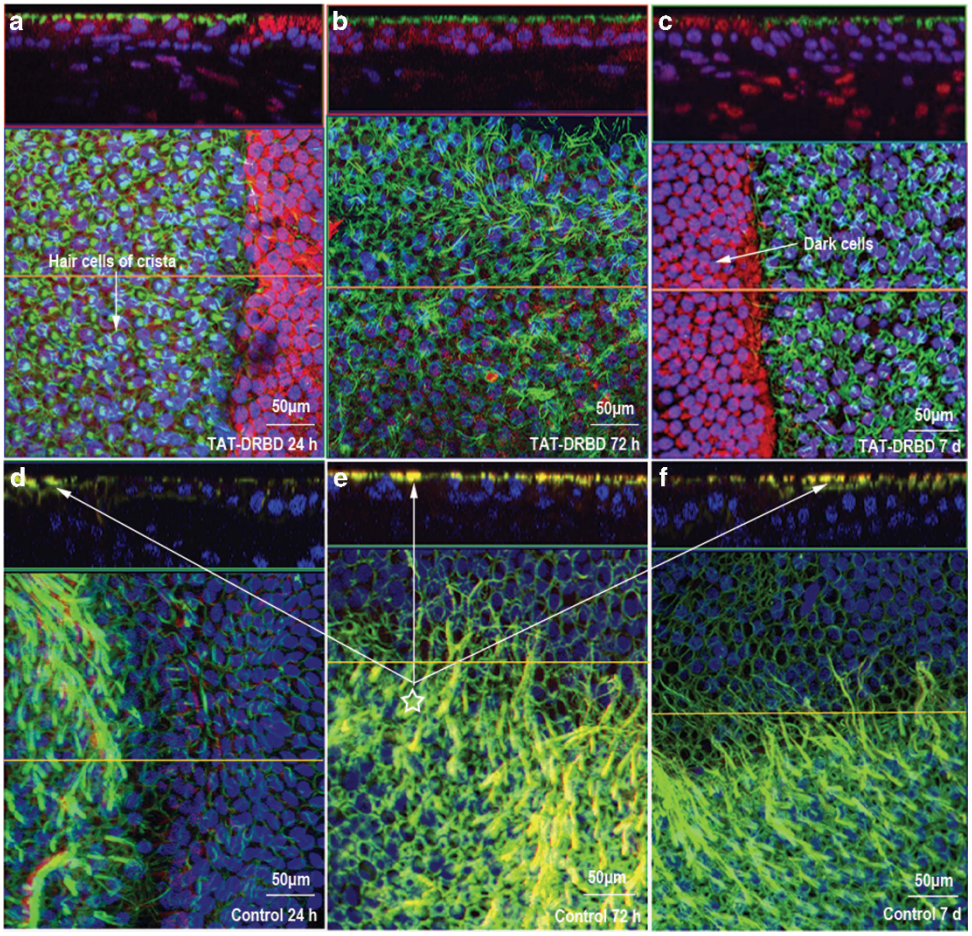

Figure 3. Crista ampullaris transfected with Cy3-labeled siRNA (red) and stained with Alexa 488 Phalloidin (green) and To-Pro-3 (blue). The shown siRNAs were successfully delivered into hair cells of the crista ampullaris with TAT-DRBD after 24 h (**a**), and siRNA uptake was greater in the dark cells on the planum semilunatum at the bottom of the crista ampullaris. Strong red fluorescence was still present after 72 h (**b**), and siRNA uptake by dark cells had not yet been eliminated after 7 days (**c**). In control ears, no siRNA was found after round-window diffusion at 24 h, 72 h and 7 days (**d**–**f**); '☆' show the red fluorescence of Cy3 was only found on membrane of hair cells but could not be found in the cytoplasm.

© 2014 Macmillan Publishers Limited

plasmids were transformed into BL21 (DE3) cells and expressed in a normal manner. The TAT-DRBD protein was obtained after a series of purifications (Figure 1b).

Cy3-labeled siRNA transfection into inner ear in chinchilla through round-window permeation with or without TAT-DRBD

To further study the specific kinetic profiles of Cy3-labeled siRNA entering the inner ear through round-window permeation, we performed an *in vivo* experiment in the chinchilla. Twenty-four hours after transfection with TAT-DRBD, the red fluorescence of Cy3-labeled siRNAs was found in the cytoplasm, of all cochlear inner hair cells and outer hair cells from the apex to the middle and basal turns (Figures 2a–c). The signal was still present after 48 h (Figure 2d) but only slightly attenuated after 7 days (Figure 2e). We did not find Cy3 fluorescence in control ears after 24 and 72 h, and 7 days (Figures 2f–h).

siRNAs were successfully delivered into hair cells of the crista ampullaris with TAT-DRBD after 24 h. siRNA uptake in dark cells on the planum semilunatum at the bottom of the crista ampullaris was markedly greater (Figure 3a). Strong red fluorescence remained evident after 72 h (Figure 3b), and siRNA uptake by dark cells had not yet been eliminated after 7 days (Figure 3c). In control ears, however, the photomicrographs showed no siRNA at 24 and 72 h, and 7 days after round-window diffusion (Figures 3d–f).

Cy3-labeled siRNAs were found in hair cells of the macula utriculi 24 h after RWM transfection. Photomicrographs showed stronger signals in peripheral dark cells (Figure 4a). We also found red fluorescence in hair cells of the macula sacculi after 24 h, but a weaker signal in the peripheral supporting the epithelium than in the macula utriculi (Figure 4d). This phenomenon can be explained by the absence of dark cells in the macula sacculi. Moreover, the dark cells may have exhibited greater phagocytosis of the siRNA/TAT-DRBD complex. siRNAs were present everywhere in the hair cells of the macula utriculi and macula sacculi after 72 h (Figures 4b and e) and remained after 7 days (Figures 4c and f), but the siRNA signal in the dark cells of the macula utriculi were eliminated quickly rather than supporting cell regions in the macula sacculi (Figures 4c and f). This indicated that either metabolism or clearance in the dark cells was more rapid. siRNAs were not found in the hair cells of the macula utriculi (Figures 5a–c) and macula sacculi (Figures 5d–f), and in the dark cells of the macula utriculi after 24 and 72 h, and 7 days in control ears.

Interestingly, strong Cy3 fluorescence was found in spiral ganglion neurons (SGNs) in the ears both with and without TAT-DRBD-mediated transfection after 24 h (Figures 6a and d), 72 h (Figures 6b and e) and 7 days (Figures 6c and f). siRNAs were

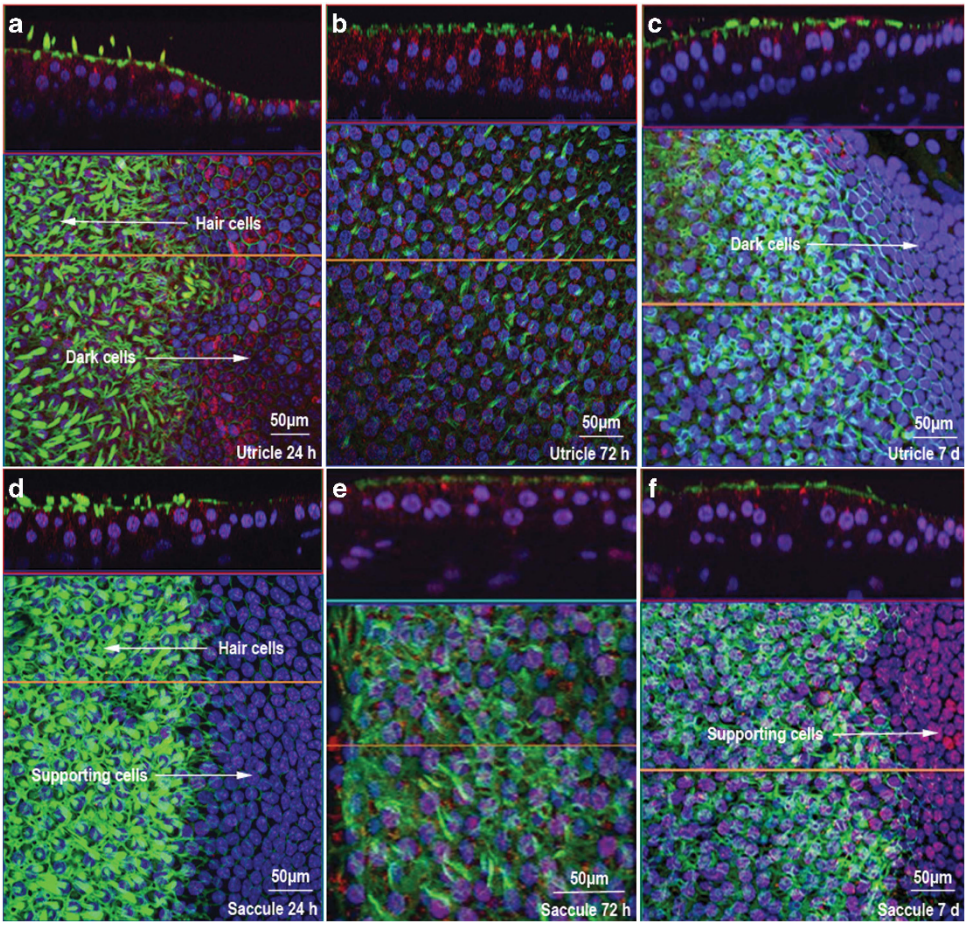

Figure 4. The macula utriculi and macula sacculi were transfected with Cy3-siRNA/TAT-DRBD through the RWM and stained with Alexa 488 Phalloidin (green) and To-Pro-3 (blue). Cy3-siRNAs are shown in the hair cells of the macula utriculi after 24 h with a stronger signal in peripheral dark cells (**a**). Cy3 fluorescence was also visible in hair cells of the macula sacculi after 24 h, but a weaker signal was present in the peripheral supporting epithelium than in the macula utriculi (**d**). This can be explained by the absence of dark cells in the macula sacculi. siRNAs were present everywhere in the hair cells of the macula utriculi and macula sacculi after 72 h (**b**, **e**) and still existed after 7 days (**c**, **f**), but the siRNA signal in the dark cells of the macula utriculi eliminated quickly than supporting cells region in the macula sacculi.

© 2014 Macmillan Publishers Limited

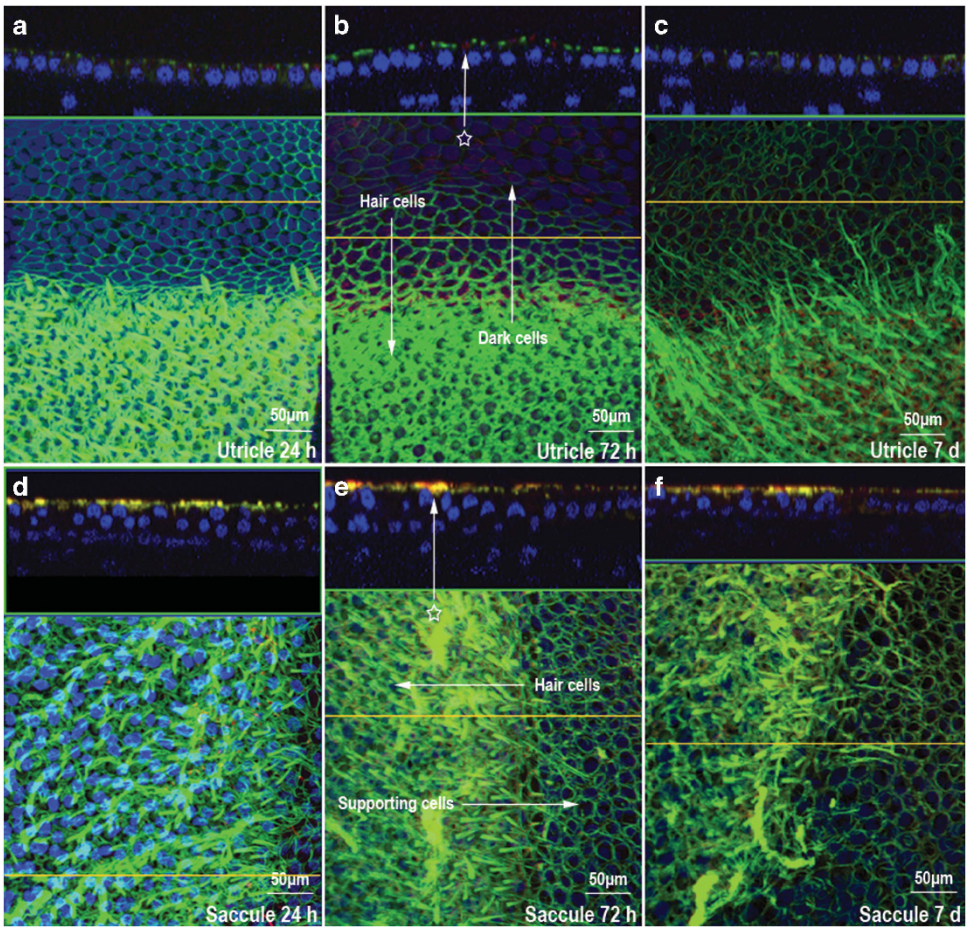

Figure 5. The macula utriculi and macula sacculi of the control ears were transfected with Cy3-labeled siRNA (red) and stained with Alexa Fluor 488 Phalloidin (green) and To-Pro-3 (blue). Cy3-siRNAs were not visible in the hair cells of the macula utriculi (**a**–**c**) and macula sacculi (**d**–**f**), as well as in the dark cells of the macula utriculi, after 24 h, 72 h and 7 days; '☆' show the red fluorescence of Cy3 was only found on membrane of hair cells, dark cell area, supporting cell region but could not be found in the cytoplasm from longitudinal section photomicrographs.

delivered into almost all SGNs after 24 h and remained evident after 7 days. A similar situation occurred in the stria vascularis; a small amount of fluorescence was detected in the epithelial cells of the stria vascularis 24 h after transfection in ears both with and without TAT-DRBD, and relatively intense fluorescence was observed in fibrocytes of the dorsal side of the spiral ligament, indicating that the siRNA delivery to the stria vascularis occurred through diffusion via the dorsal side of the spiral ligament (Figures 7a and d). After 72 h, Cy3-labeled siRNAs were present inside all epithelial cells of the stria vascularis (Figures 7b and e) but were obviously attenuated after 7 days (Figures 7c and f).

DISCUSSION

Intratympanic drugs enter the inner ear fluids primarily through the RWM. This three-layered structure comprises an outer epithelium, a connective tissue middle layer and an inner epithelium that is in contact with perilymph.[11,12,31] The outer squamous epithelial layer faces the middle ear cavity and comprises one or two layers of low cuboidal cells with tight junctions at their surface and extensive interdigitations; these cells are contiguous with the epithelium of the middle ear. The middle layer contains fibrocytes, fibroblasts, collagen fibers, elastic fibers, vessels, lymphatic channels and both myelinated and unmyelinated nerves. The density of elastin, fibroblasts and collagen increases from the middle ear surface toward the inner ear surface of the membrane. This layer is divided roughly into thirds and varies by fiber type and density, creating a gradient effect.[31] The inner layer consists of mesothelial cells contiguous with the lining of the scala tympani; cellular extensions are connected by gap junctions with long, lateral extensions and large spaces between cells. This architecture allows portions of the middle connective tissue layer to be in direct contact with the perilymphatic space. The scala tympani is filled with perilymph, which communicates with the scala vestibuli at the apex of the cochlea through the helicotrema. The perilymph of the scala tympani can be thought of as beginning at the base of the cochlea near the RWM, continuing apically to the end of the tube where it then connects with the perilymph of the scala vestibuli, and continuing back down to the base to the oval window, where the footplate of the stapes is located.[10] Using implanted electrodes and tracer ions, the longitudinal volume flow in the scala tympani was determined to be negligible, $\sim 1.6\,\mathrm{nl\,min^{-1}}$ directed apically;[32] thus, drug transport in the scala tympani, mainly through simple diffusion and along the length of the perilymphatic space, would require hours for an appropriate distribution.[10]

In this study, the fact that Cy3-labeled siRNAs were visible in the SGN and stria vascularis without TAT-DRBD indicated that siRNAs can directly permeate the RWM and enter the scala tympani in the chinchilla. As most of the structures of the cochlea are in diffusional continuity with the perilymph, siRNAs placed into the perilymph can diffuse into the organ of Corti, which contains hair cells, neuronal terminals and other specialized cells. The perilymph is also in free communication with the spiral ganglion and structures

© 2014 Macmillan Publishers Limited

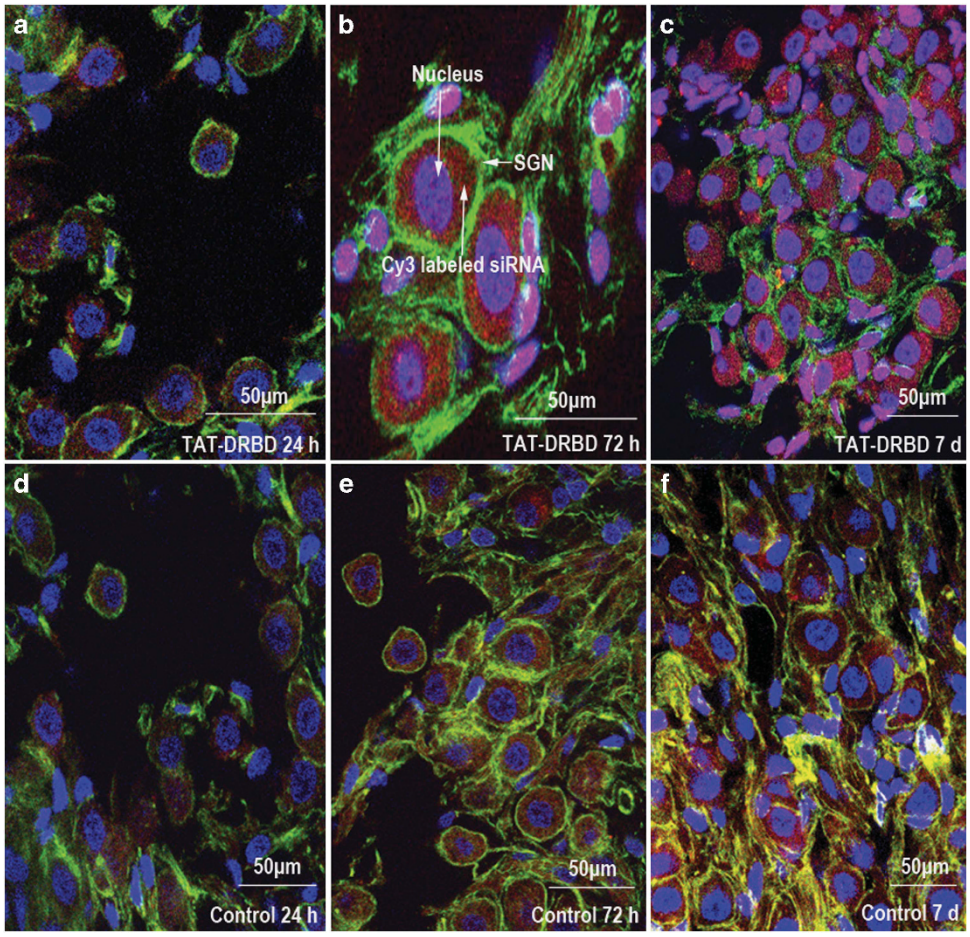

Figure 6. SGNs were transfected with Cy3-labeled siRNA (red) through the RWM and labeled by NF200/TRITC (green) and To-Pro-3 (blue). Strong Cy3 fluorescence was found in SGNs in ears both with and without TAT-DRBD after 24 h (**a**, **d**), 72 h (**b**, **e**) and 7 days (**c**, **f**). siRNAs were delivered into almost all SGNs after 24 h and remained evident after 7 days.

within the modulus via the lacuna canaliculi.[33,34] This may explain why Cy3 fluorescence was detected in the SGNs. However, in most neuronal cells siRNA delivery requires the aid of a transfection reagent.[35] The reason for the high efficiency (almost 100%) of siRNA transfection without TAT-DRBD in this study is not clear.

To date, the information available regarding diffusion between the stria vascularis and RWM is limited. The current hypothesis holds that the stria vascularis is not accessible from the perilymph.[36] The epithelium of the stria vascularis is located in the lateral wall of the scala media, which is the only epithelium with intraepithelial vessels, and generates a high potassium concentration and positive potential.[37] The cells are connected by tight junctions with separate perilymph and endolymph spaces, and are the dominant component of the blood–cochlear barrier. Interestingly, Cy3-labeled siRNAs were visible in almost all cells 24 h after transfection in the stria vascularis in ears both with and without TAT-DRBD. Few studies have demonstrated communication between the perilymph and the spiral ligament, which suggests radial communication within the cochlea. The intracellular space of the spiral ligament, which is located in the dorsolateral aspect of the stria vascularis, has a loose, fibrous structure and is filled with perilymph connected to the scala media along the inferior margin of the spiral ligament.[38–40] Figure 7a shows relatively intensive fluorescence in the fibrocytes of the dorsal side of the spiral ligament 24 h after transfection. This suggests that siRNA delivery to the stria vascularis occurred through permeation via the dorsal side of the spiral ligament in this study.

Cochlear hair cells are highly specialized neuroepithelial cells immersed in two electrochemically distinct extracellular fluids. Their basolateral membranes are immersed in perilymph of the scala tympani, whereas apical membranes are bathed in endolymph. Tight junctions couple all cells lining the endolymphatic space, limiting paracellular ion movements between the endolymph and perilymph. siRNAs were shown to be present in inner and outer hair cells after 24 h with TAT-DRBD in our experiments, but nothing was found without TAT-DRBD, indicating that the siRNA/TAT-DRBD complex passed directly through the RMW, and demonstrating the crucial role of TAT-DRBD in transfection of hair cells. Drugs in the perilymph can reach the organ of Corti via two pathways: by diffusing directly through the basilar membrane or via the osseous spiral lamina and open intercellular spaces. Indeed, a major pathway consisting of a system of canals and intercellular spaces connects the scala tympani with the intraorgan compartments.[41]

It should be noted that terminal organs of the vestibular system, including the crista ampullaris, macula utriculi and macula sacculi, are located in the scala media and are not in direct contact with the perilymph. Zou *et al.*[40] reported that tracers are rapidly taken up from the RWM to the vestibulum and the semicircular canals without passing the helicotrema, indicating an unknown radial pathway through the perilymph within cochlear fluid compartments. Substances also distribute readily through the perilymph fluid spaces of the spiral ligament into the scala vestibuli and the vestibule,[42] and nano-sized material can enter vestibular hair cells and dark cells from the intact RWM.[43] We observed a strong siRNA signal inside hair cells at the crista ampullaris, macula utriculi and macula sacculi with TAT-DRBD 24 h

© 2014 Macmillan Publishers Limited

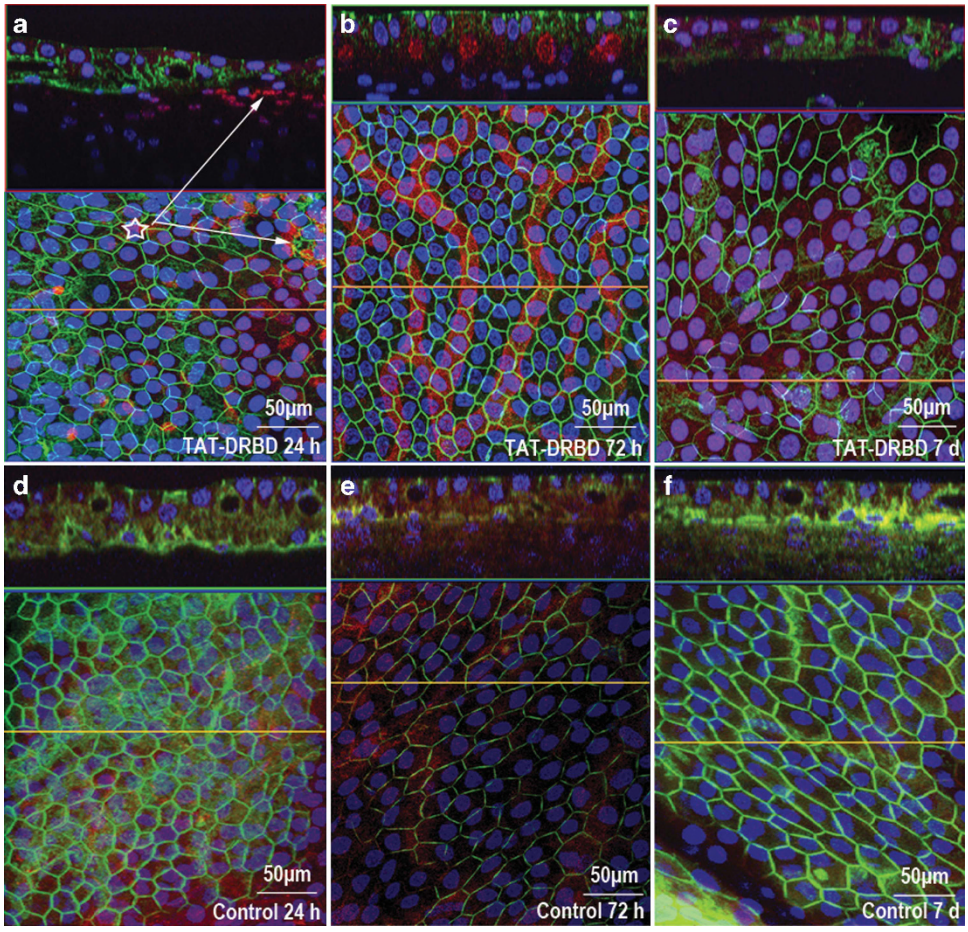

Figure 7. Stria vascularis transfection with Cy3-labeled siRNA (red) through the RWM stained with Alexa 488 Phalloidin (green) and To-Pro-3 (blue). Low-level Cy3 fluorescence was present in epithelial cells of the stria vascularis after 24 h in ears with and without TAT-DRBD, and relatively intensive fluorescence was detected in fibrocytes of the dorsal side of the spiral ligament('☆'), suggesting the siRNA delivery to the stria vascularis occurred through diffusion via the dorsal side of the spiral ligament (**a**, **d**). After 72 h, Cy3-labeled siRNAs were present inside all epithelial cells of the stria vascularis (**b**, **e**) but were obviously attenuated after 7 days (**c**, **f**).

after transfection, whereas nothing was found without TAT-DRBD, suggesting that the siRNA/TAT-DRBD complex could enter the vestibule and that TAT-DRBD was necessary for siRNA transfection. Moreover, siRNA uptake was greater by dark cells than hair cells at the crista ampullaris and macula utriculi, but lower by the peripheral supporting epithelium at the macula sacculi. This phenomenon can be explained by the absence of dark cells in the macula sacculi[44,45] or by the fact that the dark cells show greater phagocytosis of the siRNA/TAT-DRBD complexes. As dark cells and hair cells in the vestibular system are isolated from the perilymph, because the bottom of dark cells and hair cells are surrounded by supporting cells, however, the cuticular plate of dark cells and hair cells has physical contact with the endolymph that is the major approach for cellular ion exchange or material exchange. Therefore, the findings of siRNA/TAT-DRBD complexes in dark cells and hair cells in the vestibular system are believed to be absorbed by cells from the endolymph fluid.

RNAi has become a popular tool for downregulating expression of specific genes and represents a potential therapeutic strategy to preserve hearing. This technique has great potential in the fields of ototoxicity, noise-induced hearing loss, radiation ototoxicity, autoimmune inner ear disease, hereditary deafness, cell cycle regulation, signal transduction and functional genomics studies. In this study, by RWM permeation in the chinchilla *in vivo* with Cy3-labeled siRNA or siRNA/TAT-DRBD complexes, we illustrated that TAT-DRBD could transform Cy3-labeled siRNA into cells of the inner ear, including the inner and outer hair cells, crista ampullaris, macula utriculi and macula sacculi, and there was no apparent morphological damage for the time of observation. The results also demonstrate that Cy3-labeled siRNA can directly enter SGNs and the epithelium of the stria vascularis independently of TAT-DRBD from the intact RWM in the chinchilla, although the mechanism is unknown. Therefore, as a non-viral vector, TAT-DRBD, has great potential for siRNA delivery to the cochlea, which is of functional importance in suppression of the expression of specific genes in the inner ear for both research and clinical applications.

MATERIALS AND METHODS

TAT-DRBD fusion protein design, construction and purification

The DNA sequence of TAT-DRBD fusion protein (Figure 1) was synthesized and cloned into the linearized PET30a vector by a seamless method using NovoRec PCR One-Step kits (Novoprotein Scientific Inc., Shanghai, China; catalog number NR001). Competent *E. coli* DH5α cells were transformed. After sequencing was confirmed, positive plasmids were transformed into BL21 (DE3) cells. The cultures were grown at 37 °C on Luria-Bertani broth media, underwent 250 r.p.m. shaking cultivation to $OD_{600} = 0.5–0.6$ and were then induced using 1 mM isopropyl β-D-1-thiogalactopyranoside for 3 h. Cells were collected by centrifugation and lysed by ultrasonication in lysis buffer (20 mM phosphate buffer (PB), pH 7.4). Inclusion bodies were dissolved with solubilization buffer (20 mM PB, 2 M NaCl, 20 mM imidazole,

© 2014 Macmillan Publishers Limited

pH 7.4). The inclusion body solution was purified with a chelating FF(Ni) column (equilibrium buffer: 8 M urea, 20 mM Tris, 250 mM NaCl, 20 mM imidazole, pH 8.0; wash buffer: 8 M urea, 20 mM Tris, 250 mM NaCl, 50 mM imidazole, pH 8.0; elution buffer: 8 M urea, 20 mM Tris, 250 mM NaCl, 250 mM imidazole, pH 8.0). The purified inclusion body solution was added to a refolding buffer (50 mM Tris-HCl, 240 mM NaCl, 10 mM KCl, 1 mM EDTA, 0.05% PEG4000, 1 mM dithiothreitol, pH 8.2) and incubated at 4 °C for 16 h, then dialyzed against equilibrium buffer (pH 7.5) and purified using a chelating FF(Ni) column (equilibrium buffer: 20 mM PB, 2 M NaCl, pH 8.0; elution buffer: 20 mM PB, 2 M NaCl, 500 mM imidazole, pH 8.0). Finally, the eluates were combined, dialyzed against 20 mM PB and 2 M NaCl (pH 7.5), and stored at − 80 °C.

Animals and surgical procedure

Six normal adult chinchillas (560–720 g, including both males and females, 1–3 years of age, from Plymouth, OH, USA) were randomly divided into three groups (24 h, 72 h and 7 days). The right ear of each animal was prepared for local application of Cy3-labeled siRNA/TAT-DRBD onto the intact RWM and the left ear was treated with the same volume of Cy3-labeled siRNA as a self control.

Mixed TAT-DRBD and Cy3-labeled siRNA (RiboBio, Guangzhou, China; siN05815122149-1) consisted of 40 μl of 10 μM Cy3-labeled siRNA in ddH_2O added to 160 μl of 5.5–6 μM TAT-DRBD in phosphate-buffered saline (PBS) at room temperature for 30 min for the experimental right ear, and 40 μl of 10 μM Cy3-labeled siRNA in ddH_2O added to 160 μl of PBS for the control left ear.

The chinchillas were anesthetized with isoflurane (5% induction, 3% maintenance) and placed on a temperature-controlled heating pad with a rectal probe to maintain a core temperature of 37 °C. The animals were positioned in a standard stereotaxic frame and the head was held in place with ear bars. Under sterile conditions, the right bulla was exposed via a dorsal lateral approach. A 20-μl drop of Cy3-labeled siRNA (2 μM)/TAT-DRBD (5 μM) was placed onto the RWM using a microliter syringe (25 μl; Hamilton, Bonaduz, Switzerland) with the aid of a surgical microscope. After local administration, the RWM was kept in a horizontal position for 30 min. The bulla was then closed with dental cement and the wound was closed with suture material.

Histology

The chinchillas were decapitated 24 h, 72 h and 7 days after surgery. The temporal bones were removed and fixed with 10% formalin in PBS at 4 °C overnight for further preparation for histological observation. After fixation, the whole membranous labyrinth was microdissected out as described in our previous publications.[46] The entire basilar membrane, cochlear lateral wall and vestibular end organs were stained with Alex Fluor 488 Phalloidin (Invitrogen, Carlsbad, CA, USA; A12379, 1:200 in PBS) for 30 min. Some samples were double stained with To-Pro-3 (Invitrogen; T3605) for 30 min to visualize the nuclei. For staining of SGN, fixed specimens were rinsed in 0.01 M PBS and incubated overnight at 4 °C in a solution containing mouse anti-neurofilament 200 antibody (Sigma N0142, clone N52; Sigma, St Louis, MO, USA). The antibody was diluted to 1:100 in blocking solution (1% Triton X-100, 3% normal goat serum and 96% 0.01 M PBS). The specimens were rinsed in 0.01 M PBS three times and incubated for 2 h with a secondary antibody labeled with TRITC (goat anti-mouse IgG, Sigma T5393; Sigma) dissolved in 0.01 M PBS (1:200). Specimens were rinsed three times in 0.1 M PBS, mounted with glycerin on glass slides and coverslipped.

Specimens were examined under a confocal laser scanning microscope (LSM 510; Carl Zeiss, Oberkochen, Germany) using appropriate filters to detect Alex Fluor 488 Phalloidin (excitation: 495 nm; emission: 518 nm), Cy3 (excitation: 570 nm; emission: 650 nm), To-Pro-3 (excitation: 642 nm; emission: 661 nm) and TRITC (excitation: 550 nm; emission: 620 nm). Images were captured and analyzed using a Zeiss LSM Image Examiner (version 4.0.0.91; Carl Zeiss) and processed with Adobe Photoshop (version 10.0.1; Adobe Systems Incorporated, New York, NY, USA).

CONFLICT OF INTEREST

The authors declare no conflict of interest.

ACKNOWLEDGEMENTS

This research was supported by the Foundation of the Shanghai Municipal Education Commission (No. 10ZZ06).

REFERENCES

1 Fire A, Xu S, Montgomery MK, Kostas SA, Driver SE, Mello CC. Potent and specific genetic interference by double-stranded RNA in *Caenorhabditis elegans*. *Nature* 1998; **391**: 806–811.
2 de Fougerolles A, Vornlocher HP, Maraganore J, Lieberman J. Interfering with disease: a progress report on siRNA-based therapeutics. *Nat Rev Drug Discov* 2007; **6**: 443–453.
3 Sledz CA, Williams BR. RNA interference in biology and disease. *Blood* 2005; **106**: 787–794.
4 Hutvagner G, Simard MJ. Argonaute proteins: key players in RNA silencing. *Nat Rev Mol Cell Biol* 2008; **9**: 22–32.
5 Jinek M, Doudna JA. A three-dimensional view of the molecular machinery of RNA interference. *Nature* 2009; **457**: 405–412.
6 Bernstein E, Caudy AA, Hammond SM, Hannon GJ. Role for a bidentate ribonuclease in the initiation step of RNA interference. *Nature* 2001; **409**: 363–366.
7 Nykanen A, Haley B, Zamore PD. ATP requirements and small interfering RNA structure in the RNA interference pathway. *Cell* 2001; **107**: 309–321.
8 Aagaard L, Rossi JJ. RNAi therapeutics: principles, prospects and challenges. *Adv Drug Deliv Rev* 2007; **59**: 75–86.
9 Behlke MA. Progress towards in vivo use of siRNAs. *Mol Ther* 2006; **13**: 644–670.
10 Swan EE, Mescher MJ, Sewell WF, Tao SL, Borenstein JT. Inner ear drug delivery for auditory applications. *Adv Drug Deliv Rev* 2008; **60**: 1583–1599.
11 Bowe SN, Jacob A. Round window perfusion dynamics: implications for intracochlear therapy. *Curr Opin Otolaryngol Head Neck Surg* 2010; **18**: 377–385.
12 Goycoolea MV. Clinical aspects of round window membrane permeability under normal and pathological conditions. *Acta Otolaryngol* 2001; **121**: 437–447.
13 Hughes J, Astriab A, Yoo H, Alahari S, Liang E, Sergueev D *et al.* In vitro transport and delivery of antisense oligonucleotides. *Methods Enzymol* 2000; **313**: 342–358.
14 Spagnou S, Miller AD, Keller M. Lipidic carriers of siRNA: differences in the formulation, cellular uptake, and delivery with plasmid DNA. *Biochemistry* 2004; **43**: 13348–13356.
15 Balazs DA, Godbey W. Liposomes for use in gene delivery. *J Drug Deliv* 2011; 1–12.
16 Maeda Y, Sheffield AM, Smith RJ. Therapeutic regulation of gene expression in the inner ear using RNA interference. *Adv Otorhinolaryngol* 2009; **66**: 13–66.
17 Lv H, Zhang S, Wang B, Cui S, Yan J. Toxicity of cationic lipids and cationic polymers in gene delivery. *J Control Release* 2006; **114**: 100–109.
18 Kedmi R, Ben-Arie N, Peer D. The systemic toxicity of positively charged lipid nanoparticles and the role of Toll-like receptor 4 in immune activation. *Biomaterials* 2010; **31**: 6867–6875.
19 Gao Y, Liu XL, Li XR. Research progress on siRNA delivery with nonviral carriers. *Int J Nanomed* 2011; **6**: 1017–1025.
20 Okuda T, Kawaguchi Y, Okamoto H. Enhanced gene delivery and/or efficacy by functional peptide and protein. *Curr Topics Med Chem* 2009; **9**: 1098–1108.
21 Patel LN, Zaro JL, Shen WC. Cell penetrating peptides: intracellular pathways and pharmaceutical perspectives. *Pharma Res* 2007; **24**: 1977–1992.
22 Stewart KM, Horton KL, Kelley SO. Cell-penetrating peptides as delivery vehicles for biology and medicine. *Organ Biomol Chem* 2008; **6**: 2242–2255.
23 Eguchi A, Dowdy SF. Efficient siRNA delivery by novel PTD-DRBD fusion proteins. *Cell Cycle* 2010; **9**: 424–425.
24 Kaplan IM, Wadia JS, Dowdy SF. Cationic TAT peptide transduction domain enters cells by macropinocytosis. *J Control Release* 2005; **102**: 247–253.
25 Wadia JS, Stan RV, Dowdy SF. Transducible TAT-HA fusogenic peptide enhances escape of TAT-fusion proteins after lipid raft macropinocytosis. *Nat Med* 2004; **10**: 310–315.
26 Schwarze SR, Ho A, Vocero-Akbani A, Dowdy SF. *In vivo* protein transduction: delivery of a biologically active protein into the mouse. *Science* 1999; **285**: 1569–1572.
27 Nagahara H, Vocero-Akbani AM, Snyder EL, Ho A, Latham DG, Lissy NA *et al.* Transduction of full-length TAT fusion proteins into mammalian cells: TAT-p27Kip1 induces cell migration. *Nat Med* 1998; **4**: 1449–1452.
28 Bevilacqua PC, Cech TR. Minor-groove recognition of double-stranded RNA by the double-stranded RNA-binding domain from the RNA-activated protein kinase PKR. *Biochemistry* 1996; **35**: 9983–9994.
29 Bass BL, Hurst SR, Singer JD.. Binding properties of newly identified Xenopus proteins containing dsRNA-binding motifs. *Curr Biol* 1994; **4**: 301–314.
30 Eguchi A, Meade BR, Chang YC, Fredrickson CT, Willert K, Puri N *et al.* Efficient siRNA delivery into primary cells by a peptide transduction domain-dsRNA binding domain fusion protein. *Nat Biotechnol* 2009; **27**: 567–571.
31 Goycoolea MV, Lundman L. Round window membrane. Structure function and permeability: a review. *Microsc Res Technique* 1997; **36**: 201–211.
32 Ohyama K, Salt AN, Thalmann R. Volume flow rate of perilymph in the guinea-pig cochlea. *Hear Res* 1988; **35**: 119–129.

© 2014 Macmillan Publishers Limited

33 Shepherd RK, Colreavy MP. Surface microstructure of the perilymphatic space: implications for cochlear implants and cell- or drug-based therapies. *Arch Otolaryngol Head Neck Surg* 2004; **130**: 518–523.
34 Rask-Andersen H, Schrott-Fischer A, Pfaller K, Glueckert R. Perilymph/modiolar communication routes in the human cochlea. *Ear Hear* 2006; **27**: 457–465.
35 Karra D, Dahm R. Transfection techniques for neuronal cells. *J Neurosci* 2010; **30**: 6171–6177.
36 Wangemann P. Supporting sensory transduction: cochlear fluid homeostasis and the endocochlear potential. *J Physiol* 2006; **576**(Pt 1): 11–21.
37 Zdebik AA, Wangemann P, Jentsch TJ. Potassium ion movement in the inner ear: insights from genetic disease and mouse models. *Physiology* 2009; **24**: 307–316.
38 Saijo S, Kimura RS. Distribution of HRP in the inner ear after injection into the middle ear cavity. *Acta Otolaryngol* 1984; **97**: 593–610.
39 Duvall 3rd AJ, Quick CA, Sutherland CR. Horseradish peroxidase in the lateral cochlear wall. An electron microscopic study of transport. *Arch Otolaryngol* 1971; **93**: 304–316.
40 Zou J, Pyykko I, Bjelke B, Dastidar P, Toppila E. Communication between the perilymphatic scalae and spiral ligament visualized by in vivo MRI. *Audiol Neuro-otol* 2005; **10**: 145–152.
41 Ulfendahl M, Scarfone E, Flock A, Le Calvez S, Conradi P. Perilymphatic fluid compartments and intercellular spaces of the inner ear and the organ of Corti. *NeuroImage* 2000; **12**: 307–313.
42 Salt AN, Plontke SK. Principles of local drug delivery to the inner ear. *Audiol Neurootol* 2009; **14**: 350–360.
43 Wu X, Ding D, Jiang H, Xing X, Huang S, Liu H *et al.* Transfection using hydroxyapatite nanoparticles in the inner ear via an intact round window membrane in chinchilla. *J Nanoparticle Res* 2012; **14**: 1–13.
44 Forge A, Wright T. The molecular architecture of the inner ear. *Br Med Bull* 2002; **63**: 5–24.
45 Kimura RS. Distribution, structure, and function of dark cells in the vestibular labyrinth. *Ann Otol Rhinol Laryngol* 1969; **78**: 542–561.
46 Dalian Ding TJ, Weidong Q, Yan Q, Richard JS. *Science of the Inner Ear*. Chinese Science and Technology Press: Beijing, 2010.

This work is licensed under a Creative Commons Attribution-NonCommercial-ShareAlike 3.0 Unported License. To view a copy of this license, visit http://creativecommons.org/licenses/by-nc-sa/3.0/

© 2014 Macmillan Publishers Limited